Danmarks Tekniske Universitet

DTU

Wind Turbine Technology & Aerodynamics, 46300

Assignment 1
Blade Element Momentum Theory
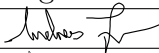
Andreas Thorsen   s144381
Nick Leenders   s192520
Ioannis Koune   s192558

4. October 2019

Note: All work has been done in the presence of all group members.

Progress Report

Name	Student nr.	Work load	Signature
Andreas	s144381	33.3 %	
Nick	s192520	33.3 %	
Ioannis	s192558	33.3 %	

All group members have contributed equally to the assignment.

The steady BEM algorithm has been implemented in Python. The script can be found in the attached zip-file. The airfoil data has been 2D-interpolated linearly using the scipy package interp2d functionality. This yields a function returning the lift and drag coefficients for a given airfoil thickness and angle of attack (AoA). The BEM has been implemented using Prandtl's tip loss correction, F and the following expression for axial and tangential induction factors

$$a_n = \frac{1}{\frac{4F \sin^2 \phi}{\sigma C_n} + 1}, \quad a_{n-1} \leq 0.33 \tag{1}$$

$$a' = \frac{1}{\frac{4F \sin \phi \cos \phi}{\sigma C_n} - 1} \tag{2}$$

For high values of a, the recommended Glauert correction for $a_{n-1} \geq 0.33$ is given by

$$C_T = 4a \left(1 - \frac{1}{4} \left(5 - 3a\right) a\right) F \tag{3}$$

has been used. Due to the nature of (3) a crude way to solve for a_n has been implemented as

$$a^* = \frac{C_{T,n-1}}{4F \left(1 - \frac{1}{4} \left(5 - 3a_{n-1}\right) a_{n-1}\right)}, \quad a_n = \beta a^* + (1 - \beta) a_{n-1} \tag{4}$$

where the second equation is a under relaxation of the results determined by β in this case to 0.1 which is needed due to the crudeness of this approach in order to assure a stable convergence. While this is simple to implement, the relaxation makes the convergence of a slow requiring more iterations. The convergence criteria has been set to an absolute difference in axial induction factor between the n'th and $n - 1$'th iteration of 10^{-5}.

Due to numerical errors arising at the tip of the blades, the tip element of the blade has been moved 0.2 [m] towards the center of the rotor for the BEM calculations. Later, when the forces are integrated, an additional integration point is added to the force and radius arrays enforcing the zero load at the tip condition. In order to validate the implementation, the total thrust and mechanical power for a wind speed of 9 m/s, a pitch angle of 0° and a rotational speed of 7.229 RPM are compared with the DTU 10MW reference report. In the report, the computed thrust is 1036 [kN] while the power is 5496 [kW]. Based on this implementation, the computed numbers are 988 [kN] and 5173 [kW], respectively. Hence, the computed loads and power are lower than the reference. However, the numbers are resembling each other, and this implementation is very basic. The error could originate from the integration of the forces which in this case has been performed using a trapezoidal numerical integration. Based on these results, the BEM implementation is deemed to be validated.

Question 1

The tip speed ratio, λ is defined as

$$\lambda = \frac{R\omega}{V_0} \tag{5}$$

where R is the rotor radius, ω is the rotational speed of the rotor and V_0 is the free stream velocity upwind of the rotor. The tip speed ratio (TSR) describes the ratio between in

the speed of the WT blade tip and the inflow velocity perpendicular to the rotor plane. It turns out that the power coefficient C_P is a function only of TSR and the blade pitch, θ_p [1] i.e. $C_P(\lambda, \theta_p)$ and hence $C_{P,opt}(\lambda_{opt}, \theta_{p,opt})$.

In order to find the optimum operational state for the Wind turbine (WT) in the region below rated power, where ω can be varied to fulfil λ_{opt}, two θ_p vs. λ grids of 40x15 points are generated. The first grid covers a large range of pitch angles from -2 to 5 degrees and TSRs ranging from 5 to 10 while the second grid is more focused and covers on the range of interest based on the previous grid saving the extra computational cost associated with a fine grid over a large range. TSR is is varied by adjusting the rotational speed while the free stream velocity is kept constant at 9 [m/s]. Calculating the corresponding C_P based on the BEM results from each grid point, a contour plot of the C_P map is created and shown in figure 6.

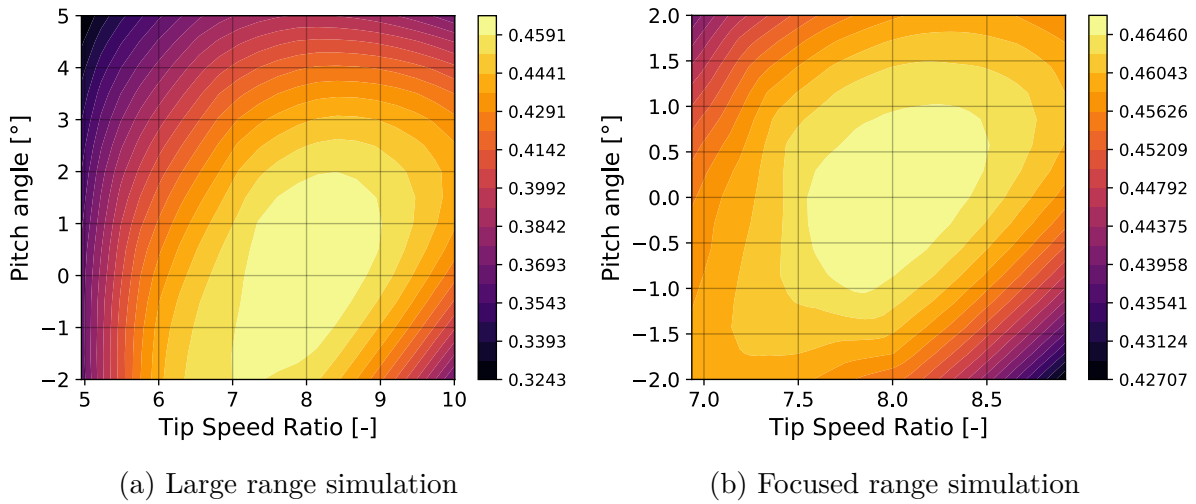(a) Large range simulation   (b) Focused range simulation

Figure 1: Contour plot of C_P for ranges of tip speed ratio and pitch angle.

It is clear from figure 1a that $C_{P,opt}$ is in the range from 7 to 9 for TSR and -2 [°] to -2 [°] in pitch angle which gives rise to figure 1b. The determined optimal point of operation with a $C_{P,opt}$ of 0.467, which seems reasonable compared to the theoretical Betz limit of ≈ 0.59, is found in table 1. Furthermore, it can be noted that the contour has very low gradients in a large area ranging from a TSR of approximately 7.5 to 8.5 and a pitch range from -1 [°] to -1 [°].

$C_{P,opt}$ [-]	λ_{opt} [-]	$\theta_{p,opt}$ [°]
0.467	8.0	0.0

Table 1: Optimal operational state below rated power

Question 2

In the previous question the optimum tip speed ratio ($\lambda_{opt} = 8.0$) and pitch angle ($\theta_{p,opt} = 0.0$ [°]) for the maximum power coefficient have already been determined. In order to ensure that the WT operates at the optimum TSR maximizing power production until

rated power is reached, the rotational speed must be varied as a function of the wind speed i.e. $\omega(V_0)$. The desired rotational speed can be determined based on (5) as

$$\omega(V_0) = \frac{V_0 \lambda_{opt}}{R} \tag{6}$$

As can be seen from the equation above, the rotational speed varies linearly with the wind speed below rated power. At some wind speed, rated power is reached and the rotational speed is kept constant for higher wind speeds. Running the BEM implementation in an iterative procedure, the rated power output of 10 [MW] is located at a wind speed of $V_{0,rated} = 11.19$ [m/s] and a rotational speed of $\omega_{rated} = 1.004$ [rad/s]. This is below the maximum allowed rotational speed of $\omega_{max} = 1.01$ [rad/s] originating from noise regulations. Based on these results, $\omega(V_0)$ has been plotted in figure 2a starting from the cut in speed of 4 [m/s] up until the cutout speed of 25 [m/s]. As can be seen in the plot, $\omega(V_0)$ the linear trend up to $[V_{0,rated}, \omega_{rated}]$ and stays constant for higher wind speeds. The results are summarized in table 2.

$V_{0,rated}$ [m/s]	ω_{rated} [rad/s]	ω_{max} [rad/s]
11.19	1.004	1.01

Table 2: Identified physical parameters at rated power.

Note that the identified power of $P_{rated} = 10$ [MW] is the mechanical power of the rotor. Since no efficiency for conversion to electric power is given, an efficiency of 100% is assumed for the conversion from mechanical to electrical power and therefore the limit is set to 10 [MW]. For values above the rated wind speed, the θ_p has to be adjusted in order to limit the amount of energy extracted from the wind. This requirement arises due to the generator being designed for a certain maximum power. Finding the appropriate pitch setting for a given wind speed will investigated in the subsequent part.
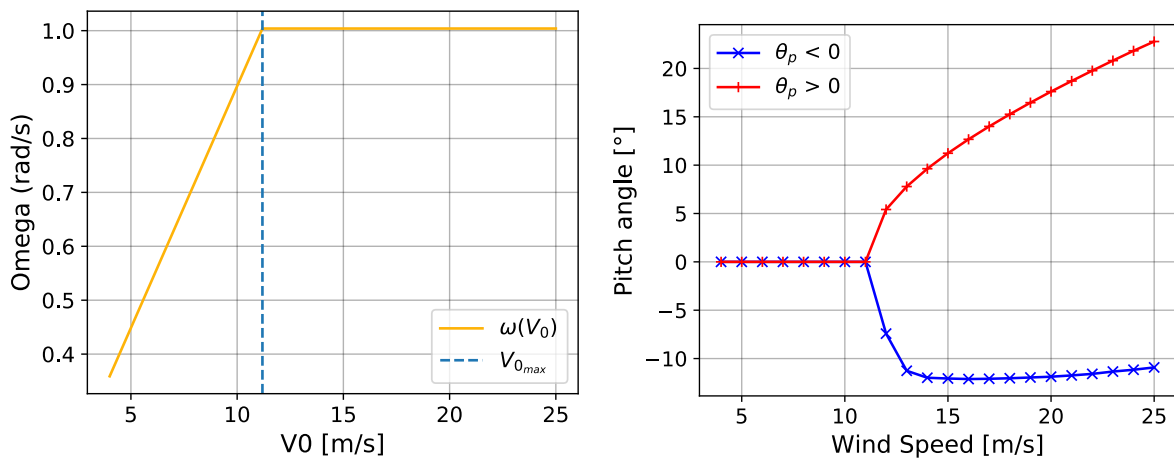
(a) Omega as a function of the free wind speed   (b) Pitch vs wind speed

Figure 2: Plot for $\omega(V_0)$ for question 2 and $\theta_p(V_0)$ for question 3

Question 3

In order to keep the power at 10 [MW] above $V_{rated} = 11.19$ [m/s], the blades are pitched. To find the appropriate pitch setting for a given wind speed, the BEM implementation is used to solve for a range of pitch settings. For all pitch settings, the resulting mechanical power is computed and compared to the desired power. The pitch setting is logged if the resulting power corresponds to the desired power with some absolute tolerance. Based on trial and error, the allowed tolerance is set to 50 [kW] corresponding to $\pm 0.5\%$ on the rated power. In order to find solutions for all wind speeds at this tolerance, the pitch range is set from -15 [°] to 25 [°] and discretized into 1500 points. The fine discretization is needed due to the high power sensitivity to pitch changes at high wind speeds. A more sophisticated, adaptive tolerance scheme could thus be used to either obtain higher accuracy of the low pitch angle settings or to reduce the number is interrogation points in the pitch angle range if a larger tolerance can be accepted at high wind speeds.

The plot in figure 2b shows the obtained results for the pitch settings. The WT runs at $\theta_{p,opt} = 0$ [°] up to V_{rated} and then splits into two branches. Clearly, two solutions exists resulting in the desired power, one with positive and one with negative pitch angle. Physically, what happens for a negative pitch is that the blade AoA increases past the onset of stall. This significantly lowers the lift coefficient for the blade but also results in increased drag. This form of pitch control is therefore designated active stall. On the other hand, increasing the pitch angle reduces the AoA and lowers both the lift and drag coefficients which is the applied control scheme for pitch regulated WTs.

(a) Power curve
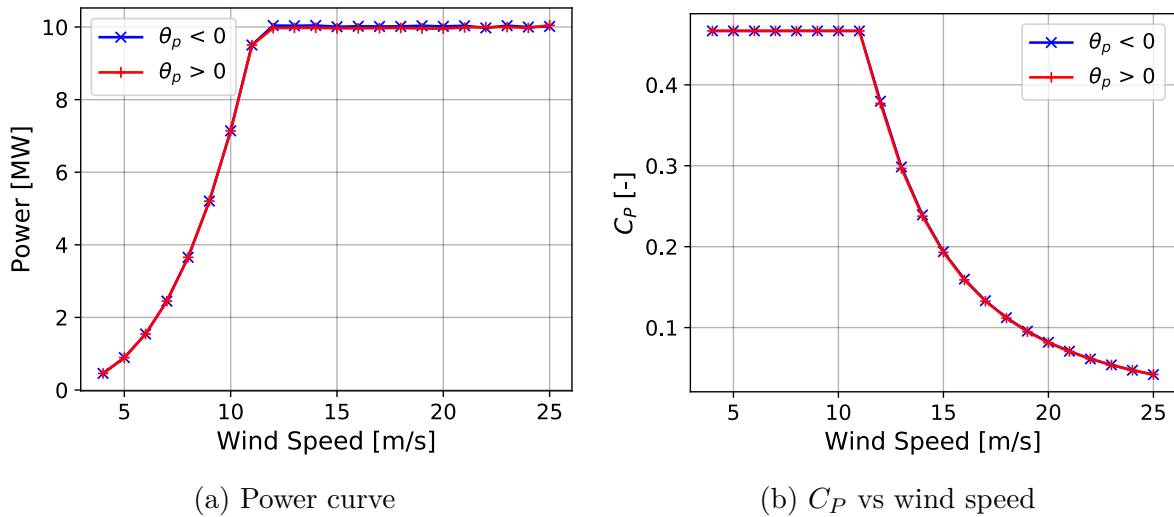
(b) C_P vs wind speed

Figure 3: Results through entire operational range for positive and negative pitch settings.

Based on the results for the pitch angles, the power and thrust curve as well as coefficients are computed and shown in figure 3 and figure 4. The power curve in figure 3a looks as expected and confirms that the power above V_{rated} is kept constant for both pitch setting solutions and varies with the wind speed cubed below rated power. Furthermore, figure 3b shows that the WT indeed operates at $C_{P,opt}$ up until rated power and declines asymptotically towards zero thereafter. However, there are distinct differences between

the two pitch strategies as seen in figure 4a and 4b. As mentioned earlier, the drag increases with AoA. As the required power is the same, the tangential forces must add up to the same rotor torque for both the positive and negative pitch case. Due to the increased drag after the onset of stall for the negative pitch case, the lift force must also increase to counter the negative tangential drag contribution, see (10). However, both lift and drag forces have a normal component which increases accordingly, resulting in a far larger thrust, see (9). While the thrust increases significantly by almost 1000 after reaching rated power for the negative pitch case followed by a slight decrease, the thrust is observed to decrease for positive pitch angles. This happens since both lift and drag is decreased with the lower AoA. Based on figure 3b and 4b and since C_P and C_T depends solely on a in the 1-D momentum theory it is also clear that the axial induction factor is constant below rated power and varies above. While the axial induction factor is diminished for the positive pitch case it would seem that it is increased based on figure 4.4 in [1] which shows $C_P(a)$ and $C_T(a)$.
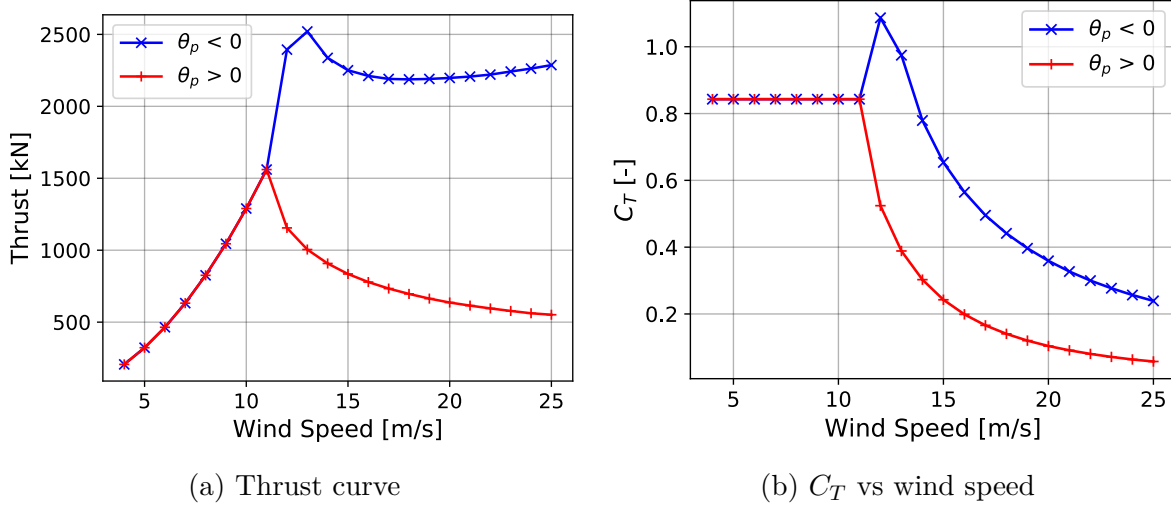

(a) Thrust curve

(b) C_T vs wind speed

Figure 4: Results through entire operational range for positive and negative pitch settings.

Question 4

The script from the previous question is executed again, where for power outputs lower than 10 [MW], the optimum pitch angle is used, whereas for wind speeds that could give an power output higher than 10 [MW] the pitch is changed to decrease the power output to 10 [MW] using either a negative or positive pitch angle. BEM is used to calculate the tangential and normal forces at all sections along the length on the blade with (7) through (10).

$$F_L = C_L\ 0.5\rho V_{rel}^2\ c \qquad (7) \qquad\qquad F_D = C_D\ 0.5\rho V_{rel}^2\ c \qquad (8)$$

$$P_n = F_L \cos(\phi) + F_D \sin(\phi) \qquad (9) \qquad\qquad P_t = F_L \sin(\phi) - F_D \cos(\phi) \qquad (10)$$

Where V_{rel} and ϕ are recalculated for each section along the length of the blade. The total bending moment around the root can be found by integrating the forces along the flade in the normal and tangential direction, respectively. The numerical integration is performed using Python's Numpy trapezoidal integral Trapz. For wind speeds of $V_0 = (4, 8, 11, 18, 25)m/s$, the total edgewise and flapwise bending moment at the root of the blade ($r = 2.8m$) are plotted in 5.

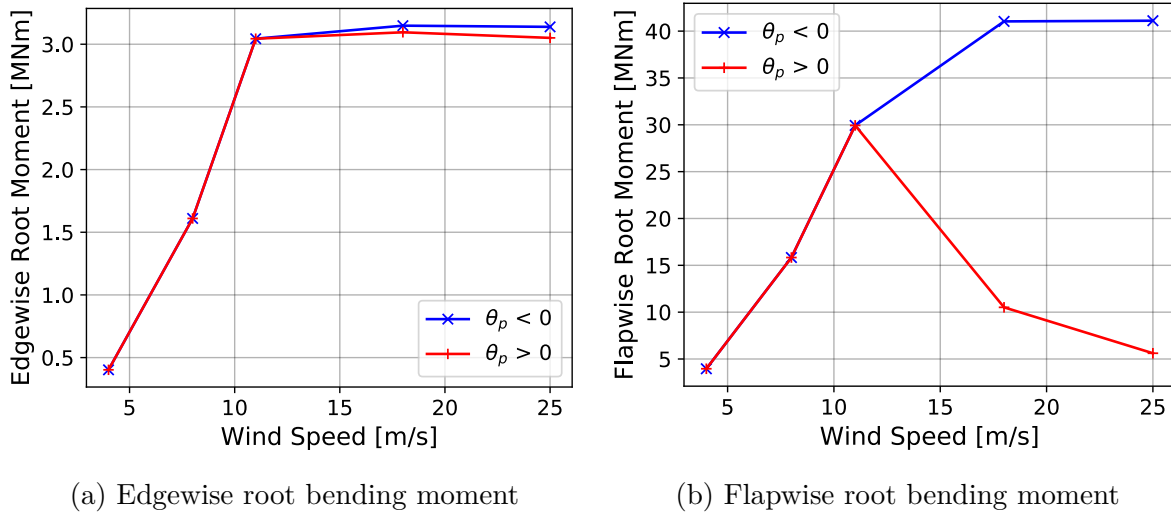(a) Edgewise root bending moment   (b) Flapwise root bending moment

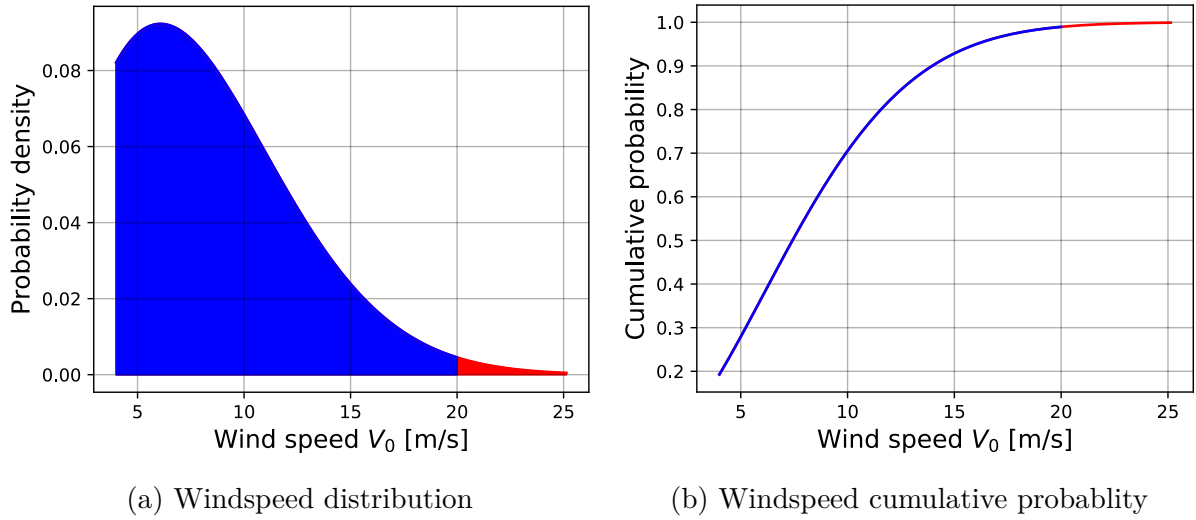Figure 5: Bending moments at the root of a rotor blade

It can be seen that for the edgewise or tangential bending moment the values are approximately the same for taking a negative or positive pitch. However, this is expected since the power output is approximately the same i.e. the required torque is the same. Also, it can be observed that the edgewise moment is much smaller than the flapwise bending moment as expected. The negative pitch angle gives much higher bending moments than the positive pitch angle. This aligns well with the results in Q3 which predict significantly higher thrust for negative pitching. Consequently, it is clear the active stall control strategy gives much higher lift and drag forces opposed to using a positive pitch to lower the AoA and thereby decrease the power. Therefore it can be concluded that it is more beneficial to use the positive pitch angle control strategy at high wind speeds, as this gives significantly lower flapwise bending moments in the blade.

Question 5

The distribution of wind speeds for the site where the wind turbine is expected to be erected is described by the Weibull parameters, $A = 9$ and $k = 1.9$. The associated probability density function, given by (11) is presented in Figure 6a. The difference between cutout speeds for $V_{out} = 25$ and $V_{out} = 20$ $[m/s]$ is also visualised.

$$f(V_0) = \frac{k}{A}(\frac{V_0}{A})^{k-1} \exp(-(\frac{V_0}{k})^k) \qquad (11)$$

(a) Windspeed distribution

(b) Windspeed cumulative probablity

Figure 6: PDF and CDF of Weibull distribution with $A = 9$ and $k = 1.9$

The annual energy output of a wind turbine can be estimated by integrating the turbine power curve over the distribution of wind velocities, in the range V_{in} to V_{out} and multiplying by the amount of hours in one year. A discrete form of the integral described above (12) can be derived using the Weibull function, which can be solved numerically in Python.

$$AEP = \sum_{i=1}^{N-1} \frac{1}{2}(P_i + P_{i+1}) \times 8760 \times [\exp(-(\frac{V_i}{A})^k) - \exp(-(\frac{V_{i+1}}{A})^k)] \qquad (12)$$

Applying the previous expression for a cutout wind speed of 25 [m/s], yields an estimate of 37.19 [GWh] for the AEP. Taking into account a reduced cutout speed of 20 [m/s] produces an AEP estimate of 36.35 [GWh]. The difference of 0.84 [GWh] (2.27 %), although not negligible, is small. This can be attributed to the fact that wind speed values at the tail of the distribution have a small probability of occurrence, as shown in Figure 6b. The exceedance probability for $V_0 = 20$ [m/s] is $P(V > V_0) \approx 0.01$.

In terms of absolute difference in AEP for the two cases, the equivalent loss in profit can be estimated. Assuming that the wind turbine operator receives 0.77 kr.[1] per kWh of power produced, the monetary loss will be 648.952 kr/turbine/year which amounts to quite some money during a lifetime of 20 years over multiple wind turbines. However, a reduced cutoff windspeed provides the advantage of lower structural strength requirements in the design, due to dynamic effects.

---

[1]Estimation based on class notes.

References

[1] M. O. L. Hansen. *Aerodynamics of Wind Turbines.* Cambridge University Press, 2015.

Appendices

A   BEMT - Python implementation

```python
# -*- coding: utf-8 -*-
```